

Article

**Design of an Oligonucleotide-Incorporated Nonfouling Surface and Its Application in Electrochemical DNA Sensors for Highly Sensitive and Sequence-Specific Detection of Target DNA**

Jiong Zhang, Ruojun Lao, Shiping Song, Zhuoyan Yan, and Chunhai Fan

*Anal. Chem.*, **2008**, 80 (23), 9029-9033 • DOI: 10.1021/ac801424y • Publication Date (Web): 31 October 2008

Downloaded from <http://pubs.acs.org> on March 20, 2009

**More About This Article**

Additional resources and features associated with this article are available within the HTML version:

- Supporting Information
- Access to high resolution figures
- Links to articles and content related to this article
- Copyright permission to reproduce figures and/or text from this article

[View the Full Text HTML](#)

# Design of an Oligonucleotide-Incorporated Nonfouling Surface and Its Application in Electrochemical DNA Sensors for Highly Sensitive and Sequence-Specific Detection of Target DNA

Jiong Zhang, Ruojun Lao, Shiping Song, Zhuoyan Yan, and Chunhai Fan\*

Shanghai Institute of Applied Physics, Chinese Academy of Sciences, Shanghai 201800, China

In this work, we report a novel electrochemical DNA sensor based on a nonfouling monolayer structure self-assembled at gold surfaces. Self-assembled monolayers (SAMs) with oligo(ethylene glycol) (OEG)-terminated thiols are known to be highly protein-resistant and effectively repel nonspecific adsorption. We found that a mixed SAM structure incorporating thiolated oligonucleotides and OEG thiols (SH–DNA/OEG) exhibited the similar nonfouling feature. More importantly, it allowed facile electron transfer across the monolayer and thus was fully compatible with electrochemical detection. On the basis of this SH–DNA/OEG platform, we developed a sandwich-type electrochemical sensor for the sequence-specific detection of DNA targets. This sensor was able to detect as little as 1 pM target DNA even in the presence of complicated biological fluids such as human serum. We also employed this sensor to directly detect a polymerase chain reaction (PCR) amplicon from the genomic DNA of *Escherichia coli* K12, which led to a very low detect limit of 60 fg (~10 copies).

There have been ever-growing interests in the development of rapid, sensitive, and cost-effective DNA sensing devices for sequence-specific detection of clinically, environmentally, or security-relevant nucleic acid targets.<sup>1–3</sup> Electrochemical DNA sensors have received particular attention due to their attractive features such as high sensitivity and fast response as well as low power/cost/mass requirements.<sup>4,5</sup> Although there have been numerous reports on electrochemical DNA sensors, their applications in the detection of unpurified samples are still poorly exploited. Among many of the reasons, the relatively simple interfacial designs at electrode surfaces usually do not satisfactorily meet the requirements of nonfouling surfaces that are resistant to nonspecific adsorption in real-world samples.

Since the invention of electrochemical DNA sensors, various strategies have been developed, aiming at the improvement of

sensitivity and selectivity of electrochemical DNA detection.<sup>6–10</sup> Among them, the “sandwich-type” strategy was popularly employed.<sup>7,11</sup> In a typical “sandwich” DNA sensor, a pair of DNA probes are designed to flank the target sequence. The capture probe is immobilized at the surface of electrodes, which brings both the target DNA and the reporter probe to the proximity of the electrode surface. After the formation of this capture probe/target/reporter probe “sandwich”, a redox moiety, which is labeled at the reporter probe and localized to the surface, produces the measurable electrochemical current signal. Clearly, DNA immobilization at the surface plays an important role in the performance of DNA sensors. Tarlov and co-workers proposed a classical interfacial design by employing a mixed self-assembled monolayer (SAM), i.e., thiolated oligonucleotides (SH–DNA), and a dilution molecule, mercaptohexanol (MCH), at gold surfaces.<sup>12–17</sup> In this design, MCH not only helps DNA oligos “stand” up at the surface, a configuration favoring subsequent DNA hybridization, but also repels nonspecific adsorption of irrelevant DNA.<sup>16</sup> SH–DNA/MCH-based electrochemical DNA sensors are able to sensitively detect DNA targets with high sequence specificity in pure DNA samples.<sup>18,19</sup> However, these sensors are still not amenable to detection in complicated samples such as polymerase chain reaction (PCR) amplicons or biological fluids.

- (6) Boon, E. M.; Ceres, D. M.; Drummond, T. G.; Hill, M. G.; Barton, J. K. *Nat. Biotechnol.* **2000**, *18*, 1318–1318.
- (7) Patolsky, F.; Lichtenstein, A.; Willner, I. *Nat. Biotechnol.* **2001**, *19*, 253–257.
- (8) Fan, C.; Plaxco, K. W.; Heeger, A. J. *Proc. Natl. Acad. Sci. U.S.A.* **2003**, *100*, 9134–9137.
- (9) Xiao, Y.; Lai, R.; Plaxco, K. W. *Nat. Protoc.* **2007**, *2*, 2875–2880.
- (10) Xiao, Y.; Lubin, A. A.; Baker, B. R.; Plaxco, K. W.; Heeger, A. J. *Proc. Natl. Acad. Sci. U.S.A.* **2006**, *103*, 16677–16680.
- (11) Yu, C. J.; Wan, Y. J.; Yowanto, H.; Li, J.; Tao, C. L.; James, M. D.; Tan, C. L.; Blackburn, G. F.; Meade, T. J. *J. Am. Chem. Soc.* **2001**, *123*, 11155–11161.
- (12) Herne, T. M.; Tarlov, M. J. *J. Am. Chem. Soc.* **1997**, *119*, 8916–8920.
- (13) Levicky, R.; Herne, T. M.; Tarlov, M. J.; Satija, S. K. *J. Am. Chem. Soc.* **1998**, *120*, 9787–9792.
- (14) Peterlinz, K. A.; Georgiadis, R. M.; Herne, T. M.; Tarlov, M. J. *J. Am. Chem. Soc.* **1997**, *119*, 3401–3402.
- (15) Petrovykh, D. Y.; Kimura-Suda, H.; Whitman, L. J.; Tarlov, M. J. *J. Am. Chem. Soc.* **2003**, *125*, 5219–5226.
- (16) Steel, A. B.; Herne, T. M.; Tarlov, M. J. *Anal. Chem.* **1998**, *70*, 4670–4677.
- (17) Steel, A. B.; Herne, T. M.; Tarlov, M. J. *Bioconjugate Chem.* **1999**, *10*, 419–423.
- (18) Steel, A. B.; Levicky, R. L.; Herne, T. M.; Tarlov, M. J. *Biophys. J.* **2000**, *79*, 975–981.
- (19) Petrovykh, D. Y.; Kimura-Suda, H.; Tarlov, M. J.; Whitman, L. J. *Langmuir* **2004**, *20*, 429–440.

\* To whom correspondence should be addressed. E-mail: fchh@sinap.ac.cn.

- (1) Heller, M. J. *Annu. Rev. Biomed. Eng.* **2002**, *4*, 129–153.
- (2) McGlennen, R. C. *Clin. Chem.* **2001**, *47*, 393–402.
- (3) Broude, N. E. *Trends Biotechnol.* **2002**, *20*, 249–256.
- (4) Drummond, T. G.; Hill, M. G.; Barton, J. K. *Nat. Biotechnol.* **2003**, *21*, 1192–1199.
- (5) Fan, C. H.; Plaxco, K. W.; Heeger, A. J. *Trends Biotechnol.* **2005**, *23*, 186–192.

**Table 1. Synthetic Oligonucleotide Probes and PCR-Amplified *E. coli* Sequences<sup>a</sup>**

Top Capture Probe (TCP)	5'SH-C <sub>6</sub> -TTTTTTTTTTTCCCACCAACGCTG 3'
Middle Capture Probe (MCP)	5'SH-C <sub>6</sub> -TTTTTTTTTCTGCATCGGCGAACT 3'
Bottom Capture Probe (BCP)	5'SH-C <sub>6</sub> -TTTTTTTTTCTGCATCGGCGAACT 3'
Top Reporter Probe (TRP)	5'ATCAATTCCACAGTTTTCGC-BIOTIN 3'
Middle Reporter Probe (MRP)	5'GATCGTTAAACTGCCTGGC-BIOTIN 3'
Bottom Reporter Probe (BRP)	5'TCCTGATTATTGACCCACAC-BIOTIN 3'
Primer 1 (P1)	5' GCGAAAACCTGTGGAATTGAT 3'
Primer 2 (P2)	5' TGATGCTCCATCACTTCTCTG 3'
Non-complementary DNA (NT)	5' AGACT TTGAT ACCAT ACTAA ATAGC ACCAT TTCCA 3'
Target DNA (T)	5' GCGAA AACTG TGGAA TTGAT CAGCG TTGGT GGGAA 3'
250bp Target DNA for <i>E. coli</i> (T250)	5' <u>GCGAA AACTG TGGAA TTGAT CAGCG TTGGT GGGAA</u> <u>AGCGC GTTAC AAGAA AGCCG GGCAA TTGCT GTGCC</u> <u>AGGCA .GTTTT .AACGA .TCAGT .TCGCC .GATGC .AGATA</u> TTCGT AATTA TGCGG GCAAC GTCTG GTATC AGCGC GAAGT CTTA TACCG AAAGG TTGGG CAGGC CAGCG TATCG TGCTG CGTTT CGATG CCGTC ACTCA TTACG GCAAA <u>GTGTG .GGTCA .ATAAT .CAGGA .AGTGA .TGGAG</u> <u>CATCA</u> 3'

<sup>a</sup> Three regions of PCR-amplified *E. coli* sequences, which were complementary to top, middle, and bottom capture/reporter probes, respectively, are distinguished by solid, dot, and dash underlines.

Here, we propose a new interfacial design involving the use of oligo(ethylene glycol) (OEG)-terminated thiols that are coimmobilized with thiolated DNA capture probes (SH–DNA/OEG) at gold electrode surfaces via the gold–sulfur chemistry. Previous reports have well documented that OEG-incorporated SAMs are a kind of protein-resistant material leading to nearly nonfouling surfaces.<sup>20–26</sup> Since OEG-based SAMs are much thicker than MCH-based ones, which partially block electron transfer at the surface, as a result, the application of this protein-resistant material in electrochemical biosensors remains largely unexplored. We then designed a SH–DNA/OEG SAM interface at gold electrode surfaces and interrogated the compatibility of this design with electrochemical detection.

## EXPERIMENTAL SECTION

**Materials.** Tris-(hydroxymethyl)aminomethane was from Cxbio Biotechnology Ltd. Ethylenediaminetetraacetic acid (EDTA), MCH, and tris(2-carboxyethyl) phosphine hydrochloride (TCEP) were purchased from Sigma-Aldrich (St. Louis, MO). Ethylene glycol-terminated thiol (HS–(CH<sub>2</sub>)<sub>11</sub>–EG<sub>2</sub>–OH, OEG) was purchased from Prochimia (Poland). TMB substrate (TMB = 3,3',5,5'-tetramethylbenzidine; Neogen K-blue low-activity substrate) was from Neogen (U.S.A.). Avidin–HRP

(horseradish peroxidase) was from Roche Diagnostics (Mannheim, Germany). The buffer solutions involved in this study are as follows: The hybridization buffer was 1 M NaCl and 10 mM TE buffer (pH 7.4). The buffer for electrochemical DNA quantification was 10 mM Tris–HCl solution (pH 7.4), and that for hybridization measurement was TMB substrate. The DNA immobilization buffer was 10 mM Tris–HCl, 1 mM EDTA, 10 mM TCEP (pH 7.4), and 1 M NaCl. 10× PCR buffer was 100 mM Tris–HCl (pH 8.3), 500 mM KCl, 15 mM MgCl<sub>2</sub>. The washing buffer was 0.1 M NaCl and 10 mM PB buffer (pH 7.4). Enzyme diluent was 0.1 M PBS buffer with 0.5% casein (pH 7.2). All solutions were prepared with Milli-Q water (18 MΩ·cm resistivity) from a Millipore system.

All synthetic oligonucleotides were purchased from Sangon Inc. (Shanghai, China). The sequences of thiol-tethered capture probes and biotinylated reporter probes are listed in Table 1. The synthetic target DNA (T) was a 35-base sequence. For the detection of genomic DNA from *Escherichia coli* K12, DNA was first extracted from *E. coli* K12 genome following the published protocol,<sup>27,28</sup> and then a 250 bp sequence (T250), *uidA* gene,<sup>29</sup> was amplified via PCR amplification. Of note, in order to optimize the detection of this long target, we designed three pairs of capture and reporter probes that flanked different regions of the PCR amplicon (i.e., top, middle, and bottom, which were named based on their positions to the electrode surface).

- (20) Mrksich, M.; Sigal, G. B.; Whitesides, G. M. *Langmuir* **1995**, *11*, 4383–4385.  
(21) Mrksich, M.; Whitesides, G. M. *J. Am. Chem. Soc.* **1997**, *119*, 361–373.  
(22) Ostuni, E.; Yan, L.; Whitesides, G. M. *Colloids Surf., B* **1999**, *15*, 3–30.  
(23) Prime, K.; Whitesides, G. *Science* **1991**, *252*, 1164–1167.  
(24) Prime, K. L.; Whitesides, G. M. *J. Am. Chem. Soc.* **1993**, *115*, 10714–10721.  
(25) Boozer, C.; Chen, S. F.; Jiang, S. Y. *Langmuir* **2006**, *22*, 4694–4698.  
(26) Boozer, C.; Ladd, J.; Chen, S. F.; Yu, Q.; Homola, J.; Jiang, S. Y. *Anal. Chem.* **2004**, *76*, 6967–6972.

- (27) Bertrand, R.; Roig, B. *Water Res.* **2007**, *41*, 1280–1286.  
(28) Kai, E.; Sawata, S.; Ikebukuro, K.; Iida, T.; Honda, T.; Karube, I. *Anal. Chem.* **1999**, *71*, 796–800.  
(29) Paton, A. W.; Paton, J. C. *J. Clin. Microbiol.* **2005**, *43*, 2944–2947.

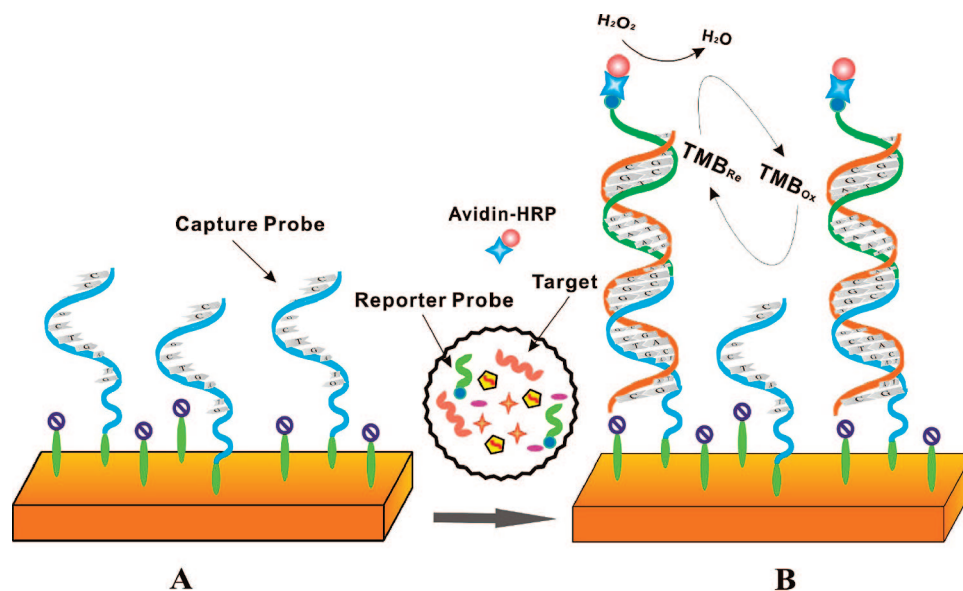


**Figure 1.** Schematic drawing for the nonfouling, SH-DNA/OEG-based electrochemical DNA sensor.

**Formation of the SAMs at Gold Electrode Surfaces.** Gold electrodes were cleaned following the reported protocol.<sup>30</sup> Briefly, gold electrodes (2 mm in diameter, CH Instruments Inc., Austin, TX) were first polished on microcloth with three different micropolish deagglomerated alumina suspensions (1.0, 0.3, and 0.05 mm in diameter) in sequence. Residual alumina powder was removed by sonicating electrodes sequentially in ethanol and Milli-Q water. Then electrodes were electrochemically cleaned in a fresh 0.5 M H<sub>2</sub>SO<sub>4</sub> solution. Finally, electrodes were rinsed Milli-Q water and then blow-dried with nitrogen. The cleaned electrodes were incubated with thiolated capture probes at appropriate concentrations in the immobilization buffer for 2 h at room temperature. The probe density was modulated by varying the concentration of capture probes (0.2, 1, 5, and 10  $\mu$ M). After that, the SH-DNA modified electrodes were treated with either 2 mM MCH or 2 mM OEG for 2 h to obtain mixed SAMs, i.e., SH-DNA/MCH or SH-DNA/OEG. Such electrodes can be stored in refrigerators for at least 1 week. Prior to the hybridization reaction, the electrodes were activated by a slight rinsing with a solution of 50 mM NaOH in 0.1 M phosphate buffer. It is worthwhile to point out that this activation step significantly increased the signal (approximately 20–30%). However, the activation mechanism remains unclear in the present stage.

**DNA Detection at Sensor Surfaces.** The 250 bp region of *E. coli* genomic DNA was amplified using a Peltier thermal cycler PTC-200 (MJ. Research Inc., SA), with the forward (P1) and the reverse (P2) primers as listed in Table 1. The final volume of the PCR reaction was 25  $\mu$ L. The temperature cycle was as follows. After a denaturation step at 95 °C for 2 min, 30-cycle amplification was performed, which consisted of denaturation at 95 °C for 30 s, annealing at 61 °C for 30 s, and extension at 72 °C for 30 s. The PCR products were diluted to 10 times with the hybridization buffer prior to the hybridization.

DNA detection of either the synthetic target or the PCR amplicon was carried out in the sandwich format. The targets were first mixed with the biotinylated reporter probe (100 nM) in the

hybridization buffer and heated to 80 °C for 5 min. The mixture was cooled to room temperature, and a 3  $\mu$ L droplet was pipetted at the sensor surface. After 1 h of incubation at room temperature, the sensor was rinsed with the washing buffer and then incubated with 2  $\mu$ L of avidin-HRP (0.5 U/mL) for 15 min at room temperature. The sensor was then extensively rinsed and subjected to electrochemical measurements.

**Electrochemical Measurements.** Electrochemical measurements were performed with either a CHI 630 electrochemical workstation (CH Instruments Inc., Austin, TX) or a homemade portable electrochemical analyzer (Figure S4 of the Supporting Information). The homemade electrochemical analyzer is 100  $\times$  60  $\times$  24 mm<sup>3</sup> in size, which employs USB to transfer the digital signal as well as provide the power supply. This portability offers the possibility of field detection. In our experiments, the small-size portable analyzer exhibited identical signals as compared to the commercial workstation. A conventional three-electrode configuration was employed all through the experiment, involving a gold working electrode, a Ag/AgCl reference electrode, and a platinum counter electrode. A glass cell with 3 mL of electrolytic buffer was placed on a cell stand. All potentials were referred to the Ag/AgCl (3 M KCl) electrode, and all measurements were carried out at room temperature. Cyclic voltammetry (CV) was carried out at a scan rate of 100 mV/s. Amperometric detection was performed with a fixed potential of 150 mV, and the steady state was usually reached and recorded within 100 s.

## RESULTS AND DISCUSSION

A biotinylated reporter probe was employed to pair with the capture probe to form a “sandwich” structure at the electrode surface (Figure 1). As a result, the biotin tag was localized at the surface, which further brought the avidin-HRP conjugate to the proximity of the surface via the strong biotin-avidin interaction. The HRP enzyme efficiently catalyzed the reduction of hydrogen peroxide with the help of an electroactive cosubstrate, TMB, which

(30) Zhang, J.; Song, S.; Wang, L.; Pan, D.; Fan, C. *Nat. Protoc.* **2007**, *2*, 2888–2895.

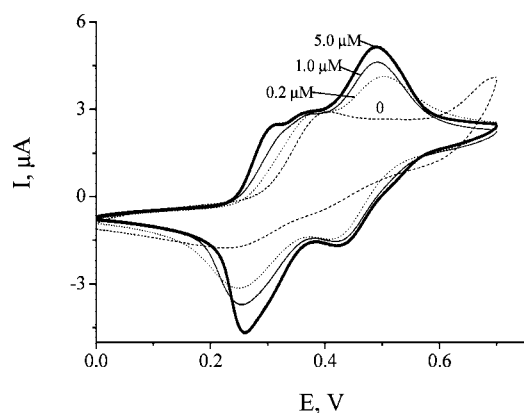


**Figure 2.** Cyclic voltammograms for the redox reaction of the TMB substrate at gold electrodes modified with 0 (dashed line), 0.2 (dotted line), 1.0 (solid line), and 5.0  $\mu\text{M}$  (thick line) thiolated DNA probe and 2 mM OEG. Scan rate: 100 mV/s.

could be readily transduced to electrochemical current signals that quantitatively reflected the amount of DNA targets.<sup>31</sup>

It is well-known that electron-transfer reactivity is critically dependent on the thickness of SAMs at electrode surfaces.<sup>32</sup> In order to evaluate whether it is possible to perform electrochemical detection at the surface of OEG-based SAMs, we interrogated the electrochemistry of TMB with a series of SAMs incorporating the OEG moiety. As shown in Figure 2, TMB exhibited a pair of poorly defined redox peaks at the surface of a pure OEG SAM, suggesting that the OEG layer blocked the electron communication between TMB and the electrode. Interestingly, we found two pairs of major redox peaks of TMB at the surface of SH–DNA/OEG SAMs, a CV pattern resembling that at bare electrode surfaces.<sup>33,34</sup> Of note, there is a small oxidation peak (0.36 V) that is slightly positive to the peak at 0.32 V, which may reflect the complicated redox reactions of TMB at the heterogeneous surface. We ascribed this effect to the penetration of TMB at SH–DNA/OEG SAMs. At the pure OEG SAM, the hydrophobic TMB molecule cannot penetrate the hydrophilic OEG layer; in contrast, positively charged TMB could bind to DNA and penetrate the DNA portion in the SAM. Indeed, we found that the more DNA molecules incorporated in the SAM, the more pronounced the CV peaks of TMB were produced (Figure 2). These results thus clearly demonstrated that the SH–DNA/OEG SAM was compatible with electrochemical measurements.

We then evaluated the protein-resistant ability of OEG-based SAMs. Two different SAMs structures, i.e., SH–DNA/MCH and SH–DNA/OEG, were prepared and compared under the same conditions. The avidin–HRP conjugate was used as the model protein since its adsorption could be electrochemically monitored. At the surface of SH–DNA/MCH, we found that avidin–HRP strongly adsorbed to the surface as reflected by the appearance of a prominent catalytic reduction peak in CV and the large increase of the amperometric current ( $\sim 3$  orders of magnitude,

Figure S1 of the Supporting Information). Of note, since biotin was not available prior to the reaction, the observed signal was purely ascribed to the nonspecific adsorption of the protein. In direct contrast, both CV and amperometric measurements showed that there was only minimal adsorption of avidin–HRP at the surface of SH–DNA/OEG, which clearly demonstrated the high protein-resistant ability. It is worth noting that the incorporation of SH–DNA made these SAMs amenable to electrochemical detection while not significantly altering the nonfouling nature of OEG. We thus concluded that the SH–DNA/OEG SAMs could serve as an electrochemical sensing platform with extremely low background and high resistant ability toward nonspecific adsorption.

By employing a synthetic DNA target of 100 pM as the model system, we investigated the performance of this electrochemical DNA sensor. After the hybridization step, we could observe a significant increase in the amperometric signal that corresponds to the catalytic reduction of  $\text{H}_2\text{O}_2$ , indicating the successful formation of the “sandwich” at the SH–DNA/OEG SAMs. Of note, it was important to add a polythymine spacer (10-T) at the 5' end of the capture probe in order to allow efficient hybridization, otherwise the specific sequence of the probe would be buried within the OEG layer.<sup>35</sup> The ratio of SH–DNA versus OEG in the SAMs strongly influenced the electrochemical signal transduction. We found that the signal was highest for the SH–DNA of 5  $\mu\text{M}$  (Figure S5 of the Supporting Information). This reflected the optimal balance between two factors, that is, the larger absolute amount of probes available at the surface led to more hybridized target, whereas the denser the SH–DNA probe spacing the lower the hybridization efficiency.<sup>35</sup>

In order to evaluate the applicability of the electrochemical DNA sensor in biological fluids, we compared its performance in pure buffer and in sera. Sera are highly complicated biological fluids containing large amounts of proteins and other molecules. Significantly, we found that the SH–DNA/OEG SAMs were highly resistant to serum, with little alteration of the background noise and nearly the same hybridization signal for the 100 pM synthetic target even in the presence of 50% serum (Figure S6 of the Supporting Information), suggesting the high protein-resistant ability of the sensor.

We challenged the sensor with the synthetic DNA target of a series of concentrations across the range of 1 pM to 10 nM. The amperometric signal was found to be a nonlinear logarithmic function related to the target concentration (Figure 3), spanning an impressive response region of 5 orders of magnitude. The detection limit was experimentally found to be at least 1 pM ( $>3$  SD, Figure S6 of the Supporting Information), which was approximately 250-fold better than that of a previously reported SH–DNA/MCH-based sensor.<sup>36</sup> This high sensitivity reflected the improved signal-to-noise ratio due to the presence of OEG. It is important to point out that all the detection was performed in the presence of 10% serum, implying that our sensor can selectively detect DNA targets in sera with a simple dilution step.

In order to test the real applicability of our sensor, we further challenged it with a 250 bp PCR amplicon (*uidA* gene<sup>29</sup>) from the *E. coli* genomic DNA. Since the 250 bp amplicon was significantly longer than the synthetic target, we first optimized

(31) Liu, G.; Wan, Y.; Gau, V.; Zhang, J.; Wang, L.; Song, S.; Fan, C. *J. Am. Chem. Soc.* **2008**, *130*, 6820–6825.

(32) Smalley, J. F.; Finklea, H. O.; Chidsey, C. E.; Linford, M. R.; Creager, S. E.; Ferraris, J. P.; Chalfant, K.; Zawodzinski, T.; Feldberg, S. W.; Newton, M. D. *J. Am. Chem. Soc.* **2003**, *125*, 2004–2013.

(33) Das, A.; Hecht, M. H. *J. Inorg. Biochem.* **2007**, *101*, 1820–1826.

(34) Fanjul-Bolado, P.; Gonzalez-Garcia, M. B.; Costa-Garcia, A. *Anal. Bioanal. Chem.* **2005**, *382*, 297–302.

(35) Wong, E. L. S.; Chow, E.; Gooding, J. J. *Langmuir* **2005**, *21*, 6957–6965.

(36) Carpini, G.; Lucarelli, F.; Marrazza, G. M. M. *Biosens. Bioelectron.* **2004**, *20*, 167–175.

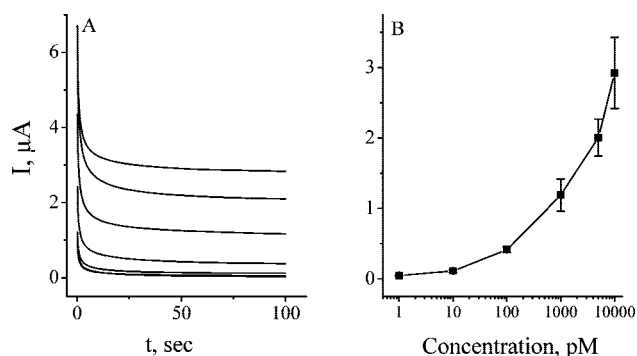


**Figure 3.** (A) Amperometric measurements for the detection of synthetic target DNA in 10% serum at a series of concentrations (from top to bottom: 10, 5, and 1 nM, 100, 10, and 1 pM, and 0). (B) Logarithmic plot of current vs target DNA concentration. Error bars show the standard deviations of measurements taken from at least three independent experiments.

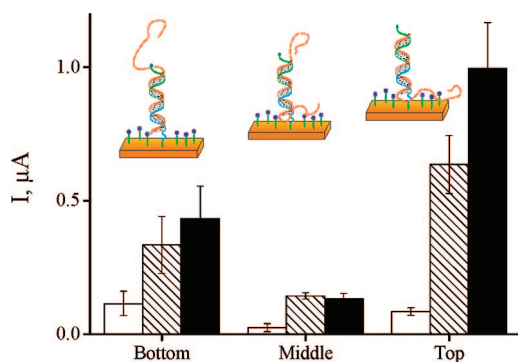


**Figure 4.** Optimization and comparison of the conditions for the sensor detection of 250 bp amplicon. Capture probes of 0.2 (unfilled), 1.0 (striped), and 5.0  $\mu\text{M}$  (filled) were employed to produce sensors with different surface densities. The capture and the reporter probes were varied from the top, to the middle, to the bottom positions of the target. The DNA template was of 0.03  $\mu\text{g}$ , and PCR reaction was performed for 30 cycles.

the position of the capture/reporter probe in order to realize best hybridization and signal transduction. We observed that the signal was highest when both probes were located at the distal end of the target (Figure 4). This is probably because the biotin label is most accessible to the avidin binding in this configuration. Again, we found that the probe concentration of 5  $\mu\text{M}$  also led to the highest signal for the long, 250 bp target. In a preliminary evaluation study of the electrochemical sensor in bacterial detection, we compared the performance of electrochemical versus electrophoretic analysis coupled with PCR amplification (Figure 5). Starting from a serially diluted *E. coli* genomic DNA, we performed PCR amplification and then measured the amplicon with either the sensor or electrophoresis. We found that the sensor could reliably detect as few as 60 fg ( $\sim 10$  copies in the 25  $\mu\text{L}$  PCR system) of *E. coli* genomic DNA when coupled with PCR, with the increase of sensitivity by 3 orders of magnitude as compared to conventional elec-

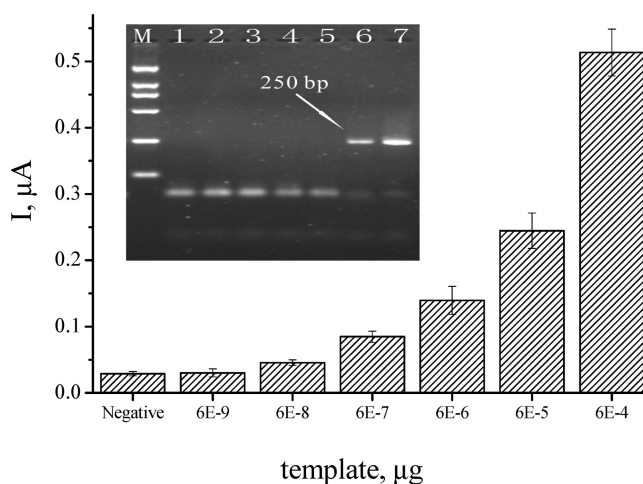


**Figure 5.** Detection of the PCR amplicon. Concentration profile for the electrochemical DNA sensor for the detection of *E. coli* genomic DNA. The DNA template was the genomic DNA extracted from *E. coli* and serially diluted by 10 times. Inset: The electrophoretic analysis of corresponding PCR products. The PCR reaction was performed for 30 cycles.

trophoresis (inset of Figure 5). Of note, we compared the performance of OEG-based and MCH-based sensors by using 600  $\mu\text{g}$  of genomic DNA and the same PCR amplification protocol. Interestingly, we found that the OEG-based nonfouling sensor generated a signal gain of  $\sim 18$ -fold, whereas it was only approximately 2-fold for the MCH-based one.

In summary, we reported a highly sensitive and selective electrochemical DNA sensor by using a novel sensor interface, SH-DNA/OEG SAMs. We demonstrated that this new interface could effectively repel nonspecific adsorption of proteins, thus serving as an ideal sensor platform for real-world applications. Importantly, we found that the presence of biological fluids such as diluted serum did not sacrifice the performance of our sensor. We also evaluated the applicability of the sensor in the detection of PCR amplicons from *E. coli* genomic DNA, which clearly showed the power of our sensor as a promising tool for the sensitive, inexpensive, and portable detection of bacterial pathogens.

#### ACKNOWLEDGMENT

This work was supported by the National Natural Science Foundation (20873175, 20725516), the Shanghai Municipal Commission for Science and Technology (0752nm021, 06ZR14106, 06ZR14136), and the Ministry of Science and Technology of China (2006CB933000, 2007CB936000, 2007AA06A406).

#### SUPPORTING INFORMATION AVAILABLE

Additional figures. This material is available free of charge via the Internet at <http://pubs.acs.org>.

Received for review July 10, 2008. Accepted September 29, 2008.

AC801424Y